Journal of Nanoscience and Technology 2(4) (2016) 197–200

ISSN: 2455-0191

Contents List available at JACS Directory

Journal of Nanoscience and Technology

journal homepage: www.jacsdirectory.com/jnst

Low-operable and Low-ppm H_2S Gas Sensing Performance of Nanocrystalline WO_3 Thin Films

J.M. Patil *

Department of Chemistry, Shri. V. S. Naik, A.C.S. College, Raver - 425508, Maharashtra, India.

ARTICLE DETAILS

Article history:
Received 26 May 2016
Accepted 02 July 2016
Available online 30 December 2016

Keywords:
Nanocrystalline WO_3
Spray Pyrolysis
H_2S Gas Sensor

ABSTRACT

Nanocrystalline WO_3 thin films were prepared by spray pyrolysis technique onto heated glass substrates with different thickness by varying spray deposition time of the solution. The structural, surface morphology, microstructural, electrical properties and gas sensing performance of the WO_3 thin films were studied on exposure of various conventional gases. As prepared thin films were characterized by employing XRD, FE-SEM, TEM and EDAX to know crystal structure, surface morphology, microstructure properties and elemental composition respectively. The crystallographic structure of the films was studied by X-ray diffraction (XRD) with crystallite size found to be 16 nm. It is found that the films are hexagonal with (110) orientation. The film was observed to be most sensitive (S = 789) to H2S at 50 °C. Furthermore, the H_2S sensor reported is cost-effective, user friendly and easy to fabricate. The quick response (6 s) and fast recovery (13 s) are the main features of this sensor.

1. Introduction

Metal oxide semiconductor chemical sensors have been a subject of intensive research due to their industrial and domestic applications in toxic and flammable gas detection [1]. Because of an increasing demand for fast and continuous detection, current research in gas sensor techniques has been focused on the development of sensors which have the characteristics of low cost, rapid response, high sensitivity, and good selectivity. The sensing mechanism is based on the surface reaction of these materials; therefore their sensing performances are strongly dependent on the morphology and structure, namely, grain size, surface area, and dimension. Especially, when the average crystallite size is smaller than or close to twice the thickness of electron depletion layer, the increase in sensor response could be even larger as the whole particle and not only the surface is fully depleted of electrons through surface interactions [2-4].

Among various metal oxides, WO_3 has found useful applications in electrochromic devices [5], semiconductor gas sensors [6], and photocatalyses [7]. Several methods have been employed to prepare nanocrystalline WO_3 thin films. These include rf magnetron sputtering [8], sol-gel [9] and chemical vapor deposition [10] are widely used for gas sensor.

Among these techniques, spray pyrolysis has proved to be simple, reproducible and inexpensive, as well as suitable for large area applications. In addition, spray pyrolysis opens up the possibility to control the film morphology and particle size in the nanometer range. Out of these approaches spray pyrolysis is a versatile technique for deposition of metal oxides [11, 12].

In the present investigations, nanocrystalline WO_3 thin films with different spraying time of the solution were prepared by spray pyrolysis technique. Structural properties, surface morphology, microstructure property and elemental composition were studied using X-ray diffraction, FE-SEM (Field effect scanning electron microscope), TEM (Transmission electron microscope) and EDAX (Energy dispersive of X-rays) respectively. These nanostructured WO_3 thin films were tested for different conventional gases.

*Corresponding Author
Email Address: jmpatil799@gmail.com (J.M. Patil)

2. Experimental Methods

2.1 Experimental Setup to Prepare Nanocrystalline WO_3 Thin Films

Fig. 1 shows spray pyrolysis set up to prepare nanocrystalline WO_3 thin films. Set-up consists of spraying chamber, substrate, spray nozzle (gun), pressure regulator, flow meter, compressor for carrier gas, heating system, precursor reservoir and temperature indicator.

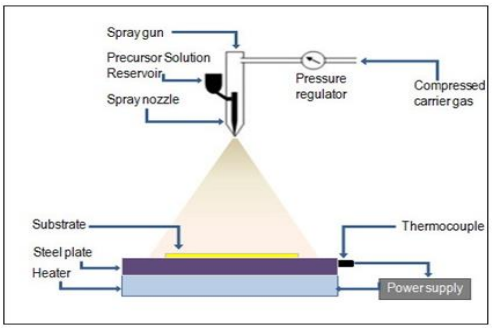

Fig. 1 Spray pyrolysis system

Table 1 Optimum parameter to obtain nanocrystalline WO_3 thin films

Deposition parameter	Optimum value / item
Spray deposition time	5 min., 10 min, and 15 min.
Nozzle-to-substrate distance	30 cm
Concentration of precursor	0.05 M
Solvent	N-N dimethyl amine
Deposition temperature	350 °C
Flow rate of solution	8 $mLmin^{-1}$

2.2 Preparation of Nanocrystalline WO_3 Thin Films

Nanocrystalline WO_3 thin films were prepared using the above set up. (0.05 M) Tungsten hexachloride (WCl_6, Purified Merck) and N-N dimethyl amine (Solvent) was chosen as the starting solution for the preparation of the films. WCl_6 and N-N dimethyl amine in 1:1 proportion were chosen for preparation of the thin films. The stock solution was delivered to nozzle with constant and uniform flow rate of 70 mL/h. by compressed air. The optimum value of spray deposition time, nozzle-to-substrate distance, concentration of precursor, deposition temperature and flow rate of solution were tabulated in Table 1. The aerosol produced by nozzle was sprayed on the glass substrate heated at 350 °C. As the prepared WO_3 thin

films samples were annealed at 500 °C for 60 min and referred as sample S1, S2, and S3 respectively. Thin films were annealed in a Muffle furnace at 500 °C for 60 minutes.

2.2 Characterization of the Thin Films

2.2.1 Determination of Film Thickness

Film thickness was measured by using a micro gravimetrical method [13] (considering the density of the bulk tungsten oxide). The films were deposited on clean glass slides whose mass was previously determined. After the deposition the substrate was again weighted, determining the quantity of deposited WO_3. Measuring the surface area of the deposited film, taking account of WO_3 specific weight of the film, thickness was determined using the relation:

$$T = M_{WO3}/A*\rho *10^4 \quad (1)$$

where A = Surface area of the film [cm^2]
M_{WO3} = Quantity of the deposited titanium dioxide
ρ = Specific weight of WO_3

The values of the film thickness are given in Table 2.

Table 2 Measurement of spray time and film thickness

Sample	Spray time (min)	Thickness (nm)
S1	5	108
S2	10	113
S3	15	124

The thickness of the film was varied from 108 to 124 nm. It was found that the thickness of the film increases with increase in deposition time of sprayed solution.

2.2.2 Structural Properties: X-Ray Diffraction Studies

The structures of the film were analyzed with X-ray diffractogram (Miniflex Model, Rigaku, Japan) using CuKα radiation with a wavelength of 1.5406 Å. The X-ray diffraction patterns were recorded from 10 to 80° as shown in Figure 2. The observed peaks: (100), (001), (110), (200), (111), (201), (401), (222) and (402) planes are very well matching with ASTM data of WO_3 [14], possessing hexagonal structure. It seen that the films exhibited strong orientation along (110). Crystallite sizes of the most sensitive samples (S2) were calculated using Scherer formula [13] which was found to be 16 nm.

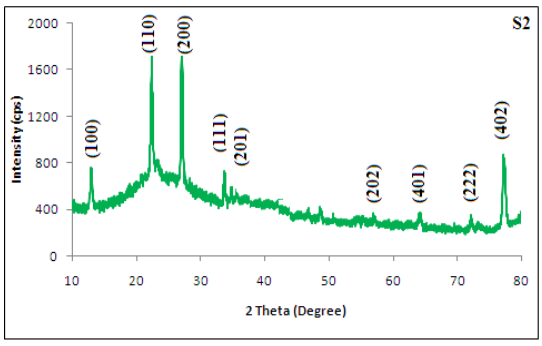

Fig. 2 X-ray diffractogram of most sensitive thin film (Sample= S2)

2.2.3 Surface Morphology

The surface morphology of the prepared film was analyzed using a field emission scanning electron microscope (FE-SEM, JEOL. JED 6300). Fig. 3 shows the FE-SEM image of most sensitive thin film sample (S2). It was observed that surface of the film was smooth and grains are spherical in nature. Grain size observed to be 21 nm.

2.2.4 Micro Structured Property using TEM and SAED Pattern

The microstructure of thin film samples was studied using transmission electron microscopy (TEM) [CM 200 Philips (200 kV HT)]. Fig. 4(a) shows the TEM image of pure WO_3, thin films obtained by scratching the thin film. The powder was dispersed in ethanol. Copper grid was used to hold the powder. It is clear from TEM image that the grains are nanocrystalline in nature and observed to be 10 nm in size.

Surface to volume ratio of such nanoparticles is very high. Therefore, these particles are highly reactive to exposed gases. The interaction between the gases and the sensitive layer is limited to the surface itself [15]. This is one of the reasons that nanostructured films give high gas response. Fig. 4(b) shows the SAED image of the S2 sample indicates high crystallanity. TEM image confirms the nanocrystalline nature of the films.

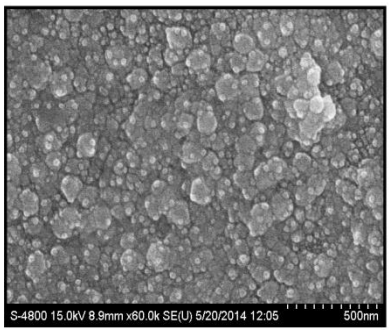

Fig. 3 FE-SEM images of most sensitive sample (S2)

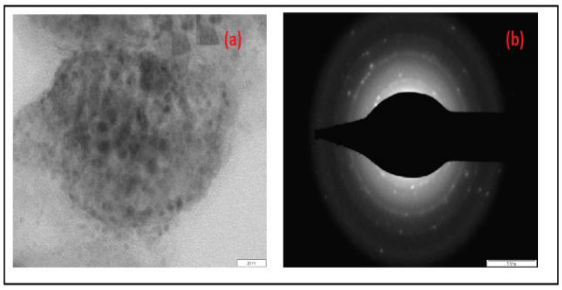

Fig. 4 TEM (a) image of most sensitive WO_3 thin film samples S2 and (b) image show electron diffraction pattern

2.2.5 Quantitative Elemental Analysis (EDAX)

Elemental composition of the prepared films was carried out at room temperature shown in Fig. 5. Table 3 shows the elemental composition of the films from EDAX. Theoretically expected stoichiometric composition of WO_3 (in terms of at %) is: W=25 % and O=75%. observed at% of W and O were tabulated in Table 3.

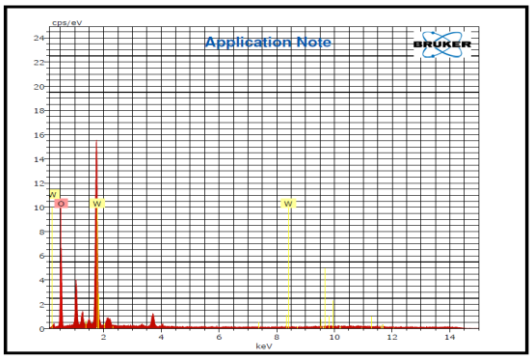

Fig. 5 Elemental analysis of the most sensitive thin film sample (S2)

Table 3 Elemental composition of the most sensitive WO_3 (Sample S2)

Element	Observed	
	wt %	at %
W	45.13	24.11
O	54.87	75.89
Total	100.00	100.00

2.3 Electrical Properties of the Sensor

2.3.1 I–V Characteristics

Fig. 6 shows I–V characteristics of nanocrystalline WO_3 thin films for the samples sprayed for 5 min, 10 min and 15 min. The graphs are observed to be symmetrical in nature indicating ohmic contact. Confirmation of ohmic contacts would ensure that the change in resistance could only be due to the influence of gas exposure.

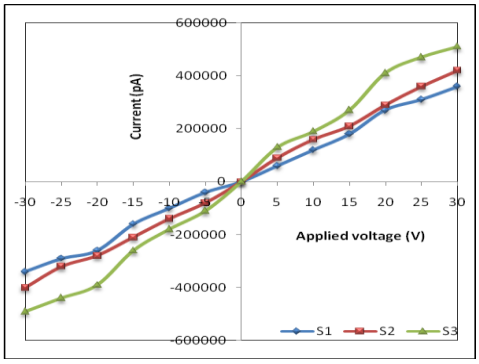

Fig. 6 I–V characteristics of nanocrystalline WO_3 thin film sensors

2.3.2 Electrical Conductivity

Fig. 7 shows the variation of log (σ) with operating temperature. The conductivity of each sample is observed to be increasing with an increase in temperature range between 50 °C and 250 °C in steps of 50 °C. The increase in conductivity with increase in temperature could be attributed to negative temperature coefficient of resistance and semiconducting nature of nanocrystalline WO_3. It is clearly indicates that the nanocrystalline WO_3 thin films were semiconducting in nature.

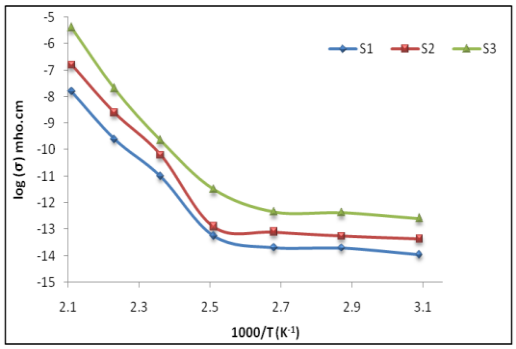

Fig. 7 Variation of log (σ) with operating temperature (°C)

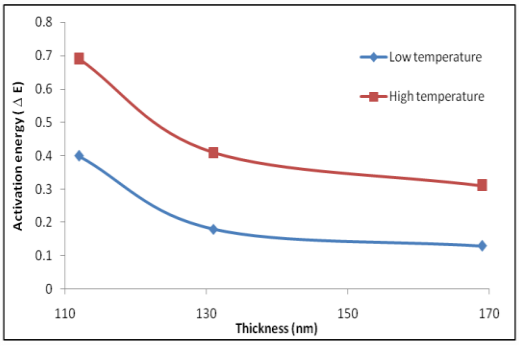

Fig. 8 Variation of activation energy (ΔE) with thickness (nm)

It is reported [16] that there is a variation of activation energy with film thickness. The activation energy calculated from the slopes of line for 5 min, 10 min, and 15 min thin films. It is observed from the Fig. 8 that as the thickness of the films increases, activation energy goes on decreases.

2.4 Gas Sensing Performance of the Sensors

2.4.1 Measurement of Gas Response

Gas response (S) of the sensor is defined as the ratio of change in current to the current of the sensor on exposure of target (at same operating conditions).

$$S = I_a\text{-}I_g/I_a \qquad (2)$$

where, I_a = the current of the sensor in air
I_g = the current on exposure of a target gas

2.4.2 Gas Response with Operating Temperature

The gas-sensing performance of the nanocrystalline thin films was tested using static gas-sensing system [13]. The heater was fixed on the base plate to heat the sample under test. Operating temperature was changed from room temperature to 500 °C. The current passing through the heating element. Cr–Al (Chromel-Alumel) thermocouple was used to sense the operating temperature of the sensor. The output of the thermocouple was connected to a digital temperature indicator. A gas inlet valve was fitted at one of the ports of the base plate. The required gas concentration inside the static system was achieved by injecting a known volume of a test gas using a gas-injecting syringe. The electrical connections were brought out from the system to connect dc voltage source and digital picoammeter. A constant voltage was applied to the sensor, and the current was measured by a digital picoammeter. The air was allowed to pass into the glass chamber before start of (every) new gas exposure cycle. The required gas concentration inside the dome was achieved by injecting predefined known volume of the test gas in chamber filled with ambient air at atmospheric pressure. Values of current before and after exposure of gas were recorded. Values of conductance were determined to obtain the gas response.

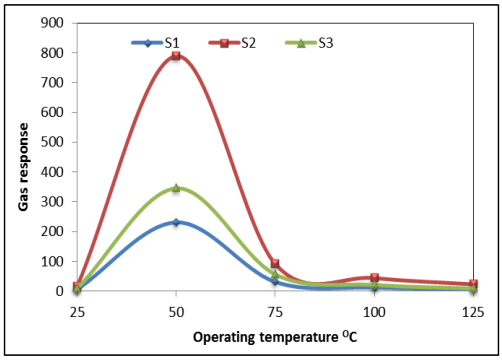

Fig. 9 Gas response of nanocrystalline WO_3 thin films with operating temperature

Fig. 9 shows variation of gas response with operating temperature of samples S1, S2 and S3 on exposure of 5 ppm H_2S. It is clear that the H_2S response of sample S2 is higher (S = 789) at 50 °C as compared to those of S1 (S = 231), S3 (S= 345). It is well-known that the response of the metal–oxide semiconductor sensors is mainly determined by the interactions between a target gas and the surface of the sensor [17].

2.4.3 Selectivity

Selectivity or specificity is defined as the ability of the sensor to respond to certain gas in the presence of the other gases. Selectivity of nanocrystalline WO_3 thin film sensors is measured at an operating temperature of 50 °C. Fig. 10 depicts the bar diagram to indicate H_2S selective ability of the sensor.

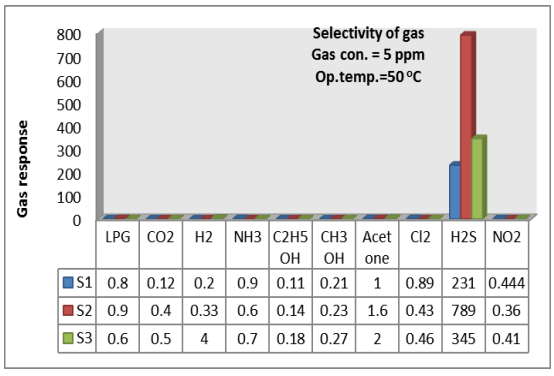

	LPG	CO2	H2	NH3	C2H5 OH	CH3 OH	Acet one	Cl2	H2S	NO2
S1	0.8	0.12	0.2	0.9	0.11	0.21	1	0.89	231	0.444
S2	0.9	0.4	0.33	0.6	0.14	0.23	1.6	0.43	789	0.36
S3	0.6	0.5	4	0.7	0.18	0.27	2	0.46	345	0.41

Fig. 10 Selectivity of nanocrystalline WO_3 thin films for different gases

2.4.4 Response and Recovery of the Sensor

The time taken for the sensor to attain 90% of the maximum decrease in resistance on exposure to the target gas is the response time. The time taken for the sensor to get back 90% of original resistance is the recovery time. The response and recovery of the nanocrystalline WO_3 thin film (S2) sensor on exposure of 5 ppm of H_2S at 100 °C are represented in Fig. 11. The response is quick (6 s) and recovery is fast (13 s). The high oxidizing

ability of adsorbed oxygen species on the surface nanoparticles and high volatility of desorbed by-products explain the quick response to H_2S and fast recovery [18].

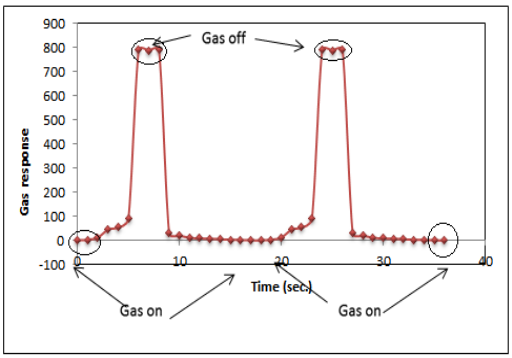

Fig. 11 Response and recovery of the sensor

3. Results and Discussion

3.1 H_2S Gas Sensing Mechanism

The gas response of any metal oxide semiconductor to a particular gas increases with the decrease in the size of nanocrystallites [19, 20] due to an increase in surface to volume ratio and therefore the reactivity. Grain sizes and microstructures of the sensor affect the gas sensing performance of the sensor. It was found that, if the grain size of the sensor material is sufficiently small, the area of active surface sites is larger, and the sensitivity and selectivity for a particular gas enhances largely. Nanocrystalline material would be expected to show much better gas sensing performance as compared with the sensor fabricated from bulk materials [20].

At low and medium temperatures (about 300 °C - 400 °C), oxygen is adsorbed on the oxide crystals surface as ions are formed by abstracting free electrons from the semiconductor solid, reducing the electrical conductivity. This reaction is described by Eq. (3)

$$O_2 + 2\,e^- \longrightarrow 2\,O^-_s \qquad (3)$$

Beside, this fact creates a monolayer of oxygen negative ions that produces a repulsion force over the free electrons inside the oxide crystal.

The resistance of the nanocrystalline WO_3 thin films decreases as gas flows into the test chamber and adsorbed on the surface of the nanocrystalline WO_3. However, when nanocrystalline WO_3 thin film consisting of nanograins in absence of H_2S, the depletion layer would extend throughout the entire layer of nanocrystalline WO_3 on the film, and its resistance would become strikingly large. In a H_2S gas environment, the depleted layer would shrink quickly as it obtains conduction electrons due to reaction between H_2S adsorbed oxygen and the resistance of the nanocrystalline WO_3 would experience a large change. The response to H_2S can be explained in the following reaction. Then, the electrons are confined in the centre of the crystals and a depletion layer is formed just below the crystal surface. So, a potential barrier appears between the oxide crystals, causing an additional reduction of the electrical conductivity. In the presence of a reducing gas (R), this gas will react with the adsorbed oxygen, leaving free the previous trapped electrons and the new molecule keeps free. This reaction is described by Eq. (4)

$$R + O^-_s \longrightarrow RO + e^- \qquad (4)$$

4. Conclusion

Nanocrystalline WO_3 thin films prepared by simple and inexpensive spray pyrolysis technique onto the glass substrates by varying spray time of precursor solution. The structural, morphological and microstructural properties confirm that the as-prepared WO_3 thin films were nanostructured in nature. The elemental analysis conferred that as prepared thin films was nonstoichiometric in nature. Thickness of the films was observed to increase from 108 to 124 nm with increase in spray time of solution. The WO_3 thin film of (Sample S2= 10 min spray time) was most sensitive to H_2S gas and exhibit the response of S= 789 to the gas concentration as 5 ppm at the low operating temperature of 50 °C. The sensor has good selectivity to H_2S against different gases. The nanocrystalline WO_3 thin films exhibit rapid response–recovery which is one of the main features of this sensor.

Acknowledgements

The authors are thankful to the University Grants Commission, New Delhi for providing financial support. Thanks to Principal, Shri. V.S. Naik A.C.S. College, Raver, for providing necessary infrastructure laboratory facilities for this work. We also appreciate Prof. Dr. R. H. Bari, Head of Department, Department of Physics, G. D. M. Arts, K. R. N. Com. And M. D. Science College, Jamner for their help. We thanks NMU, Jalgaon for the motivation and encouragement for giving me the opportunity to do this research work as successful one.

References

[1] H.R. Kim, K. Choia, J.H. Lee, S.A. Akbar, Highly sensitive and ultra-fast responding gas sensors using self-assembled hierarchical SnO_2 sphere, Sens. Actuators B 136 (2009) 138-143.
[2] G. Zhang, M. Liu, Effect of particle size and dopant on properties of SnO_2-based gas sensors, Sens. Actuators B 69 (2000) 144-152.
[3] J.M. Patil, S.B. Patil, R.H. Bari, R.T. Chaudhari, A.N. Sonar, Influence of film thickness on structural, surface morphology and electrical properties of spray pyrolise nanostructured WO_3 thin films, J. Adv. Phys. 5 (2016) 1-5.
[4] R.H. Bari, Gas sensing performance of chemically deposited nanocrystalline Cu_2S thin films, Inter. J. Technol. Chem. Res. 02 (2016) 133-140.
[5] C. Santato, M. Odziemkowski, M. Ulmann, J. Augustynski, Crystallographically oriented mesoporous WO_3 films: Synthesis, characterization, and applications, J. Amer. Chem. Soc. 123 (2001) 10639-10649.
[6] Y.S. Kim, H. Seung-Chul, K. Kim, H. Yang, S.Y. Choi, et al, Room-temperature semiconductor gas sensor based on nonstoichiometric tungsten oxide nanorod film, Appl. Phys. Lett. 86 (2005) 213105-213112.
[7] K. Sayama, K. Mukasa, R. Abe, Y. Abe, H. Arakawa, Stoichiometric water splitting into H_2 and O_2 using a mixture of two different photocatalysts and an IO_3-/I- shuttle redox mediator under visible light irradiation, Chem. Commun. 01 (2001) 2416-2423.
[8] J.L. Solis, Highly porous tungsten-oxide-based films obtained by spray-gel for gas sensing Applications, Rev. Mexicana De Fisica 52 (2006) 29-31.
[9] M. Ferroni, V. Guidi, G. Martinelli, G. Sberveglieri, Microstructural characterization of a titanium-tungsten oxide gas sensor, J. Mater. Res. 12 (1997) 793-798.
[10] V. Srivastava, A.K. Srivastava, K.N. Sood, K. Jain, Sol gel synthesis of tungsten oxide thin film in presence of surfactant for NO_2 detection, J. Sens. Transducers 107 (2009) 99-110.
[11] R.H. Bari, S.B. Patil, Nanostructured spray pyrolysis zinc doped CdO thin films for LPG gas sensor, J. Nanosci. Technol. 2(2) (2016) 104-108.
[12] J.M. Patil, S.B. Patil, R H. Bari, A.N. Sonar, Conventional gas sensor application of nanostructured WO_3 thin films, Sens. Lett. 13 (2015) 1-8.
[13] R.H. Bari, S.B. Patil, A.R. Bari, Influence of precursor concentration solution on CO sensing performance of sprayed nanocrystalline SnO_2 thin films, Optoelect. Adv. Mater. Rapid Commun. 6 (2012) 887-895.
[14] JCPDS card no. 01-075-2187.
[15] Simon, N. Barson, Micro machined metal oxide gas sensors: opportunities to improve sensor performance, Sens. Actuators B 73 (2001) 1-26.
[16] K.C. Sharma, J.C. Garg, Influence of thermal annealing in air on the electro optic characteristic of chemical bath deposited non-stoichiometric cadmium zinc selenide thin films, Phys. D: Appl. Phys. 23 (1990) 1411-1419.
[17] R. Kumar, S.A. Imam, M.R. Khan, A critical review of Taguchi gas sensor for the detection of VOC'S, MASAUM J. Rev. Surv. 1 (2009)177-183.
[18] L.A. Patil, A.R. Bari, M.D. Shinde, Vinita Deo, Ultrasonically prepared nanocrystalline ZnO thin films for highly sensitive LPG sensing, Sens. Actuators B: Chem. 149 (2010) 79-86.
[19] L.A. Patil, A.R. Bari, M.D. Shinde, Vinita Deo, Ultrasonically synthesized nanocrystalline ZnO powder based thick film sensor for ammonia sensing, Sens. Rev. 30 (2010) 290 - 296.
[20] L.A. Patil, A.R. Bari, M.D. Shinde, Vinita Deo, D.P. Amalnerkar, Synthesis of ZnO nanocrystalline powder from ultrasonic atomization technique, characterization, and its application in gas Sensing, IEEE Sens. 11 (2011) 939-946.